CLAY ALIGNMENT IN ELECTRIC FIELDS

ALINEACIÓN DE ARCILLAS EN CAMPOS ELÉCTRICOS

R. C. Castberg[a †], Z. Rozynek[b], J. O. Fossum[b,d ‡], K. J. Måløy[a,d *], P. Dommersnes[c,d] and E. G. Flekkøy[a,d]

a) Department of Physics, University of Oslo, P.O. Box 1048, NO-0316, Oslo, Norway,
rene@castberg.org†, k.j.maloy@fys.uio.no*
b) Department of Physics, NTNU, Høgskoleringen 5, NO-7491, Trondheim, jon.fossum@ntnu.no‡
c) Matieres et Systemes Complexes, Universite Paris 7, 75253, Paris, France
d) Centre for Advanced Study at the Norwegian Academy of Science and Letters, Drammensveien 78, NO-0271 Oslo, Norway
†, ‡, * corresponding authors

The response of rotational alignment of lithium fluorohectorite (Li-Fh) to an external electric field has been studied by employing image analysis. Large aggregates consisting of many single clay particles were prepared using a sedimentation technique in order to control both their shapes and sizes. Such aggregates have a layered structure which was confirmed by wide-angle X-ray scattering (WAXS) studies. Measuring the electric-field-induced alignment of these particles we obtained a data collapse by plotting $\ln(\theta)$ versus t/E^2, where θ is the rotational angle, t is time and E is the electric field strength.

Se estudia la respuesta de la alineación rotacional de la fluorohectorita de litio (Li-Fh) debido a un campo eléctrico externo mediante análisis de imágenes. Se prepararon grandes agregados consistentes en muchas partículas individuales de arcilla usando una técnica de sedimentación, con el objetivo de controlar tanto sus formas como sus tamaños. Tales agregados poseen una estructura a capas, lo que fue confirmado por dispersión de rayos X de ángulo ancho (WAXS). Midiendo el alineamiento inducido por campo eléctrico de las partículas, obtuvimos un colapso de los datos en un gráfico $\ln(\theta)$ vs. t/E^2 donde θ es el ángulo de rotación, t es el tiempo, y E es la intensidad del campo eléctrico.

PACS: Electrorheological fluids, 47.65.Gx; self-assembly (nanofabrication), 81.16.Dn; X-ray scattering in structure determination, 61.05.cf

INTRODUCTION

On application of an external electric field, clay particles suspended in non-polar and non-conductive carrier fluids (such as silicone oil) will rotate and align themselves [1] such that their stacking direction is normal to the electric field direction. Once these particles have aligned themselves, they will eventually start forming chain-like structures [2, 3, 4]. In order to understand the processes behind chain formation, we have to understand how the individual particles initially orient themselves with the field. From preliminary observations, we find that for small particles this process takes a couple of *ms*, for this reason we prepared larger particles which were easier to manipulate. In this work optical measurements were made of the particles aligning themselves in the electric field and we show that there is a E^2 dependency on the rotation rate.

SAMPLE PREPARATION

Lithium fluorohectorite (Li-Fh) was purchased from Corning Inc., New York in the form of a white powder. Li-Fh is a synthetic 2:1 smectite clay having the nominal chemical formula $Li^{+}_{1.2}[[Mg_{4.8}Li_{1.2}]Si_8O_{20}F_4]^{1.2-}$ per unit cell, where Li is an interlayer exchangeable cation (not to confuse with Li in the crystaline sheet); for more details on structure see reference [5]. Li-Fh has a surface charge of 1.2 e-/unit cell and is a polydisperse clay with platelet diameters ranging from a few hundred *nm* up to several μm [6]. In order to have a better control on the particle shape and size (parameters that may influence the rotation time when particles are subjected to *E*-fields), it was decided to prepare the samples as follows. The Li-Fh powder was mixed with deionized water and stirred for 12 *h* at RT. Next, the solution was transferred to a flat Petri dish and then left for 3 days at RT for water evaporation. During that time the individual clay particles sediment, and generally lie flat on the bottom of the dish and consequently stack on one another as sketched in Figure 2 (a). In order to obtain different particle thicknesses' four different clay concentrations were used, namely 0.5, 1, 2 and 4 *wt.*%. In this proceeding we will present data from the 2 *wt.*%. Once the samples have dried, they were carefully cut into small pieces with desired lengths and widths (see Figure 1).

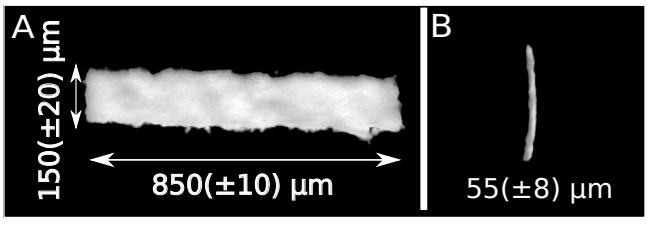

Figure 1: Optical microscopy images of the sample showing length of around 0.85 *mm* (A) and thickness of around 55 μm (B).

SAMPLE CHARACTERISATION

The sample shown in Figure 1, with thickness of around

55 μm, was measured at our home laboratory (NTNU, Norway) using a NanoSTAR X-ray instrument from Bruker AXS, setup in a wide-angle X-ray scattering (WAXS) configuration during the present experiments. This instrument is equipped with a CuKα micro-source emitting X-rays at wavelength of 1.5418 $Å$; and a 2-D detector that collects Bragg diffraction rings. The equipment enabled the investigation of both the orientational distribution of the clay platelet stacks and the characteristic interlamellar distance for monitoring the intercalated water content. The X-ray beam is directed such that it is normal to the sedimentation direction, as shown in Figure 2 (a), i.e. the thickness of the particle. The beam has a diameter of about 0.4 mm and the available scattering q-range for the setup used here was: 0.08 - 1 $Å^{-1}$.

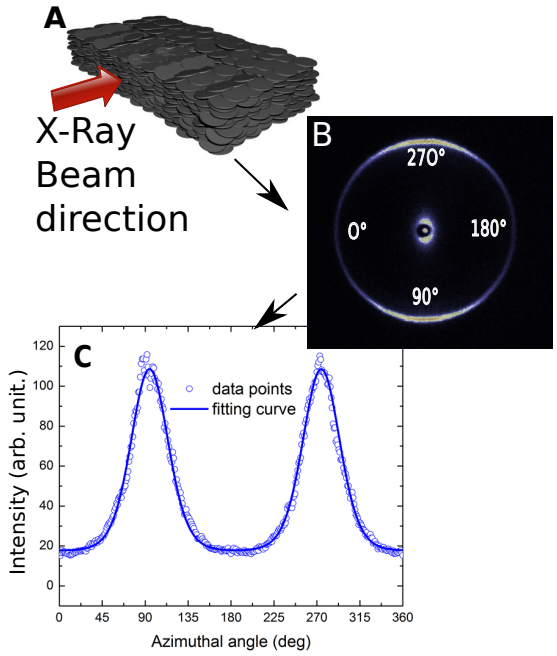

Figure 2: (A) Clay platelets forming an aggregate, (B) resulting in an asymmetry in the WAXS data. (C) The azimuthal plot is made by radial integration of the 2-D WAXS pattern. The parametric fit (solid line) is used to calculated the nematic order parameter (here $S_2 = -0.34 \pm 0.02$).

An example of the two-dimensional WAXS pattern is shown in Figure 2 (b). The 001 Bragg ring that originates from the clay interlamellar distance (between clay crystalline sheets) is anisotropic indicating that the clay particles have a preferential orientation. Since the scattering intensity peaks at 90° and 270° and the direction of the X-ray beam is horizontal, one can conclude that the clay particles are oriented with their stacking direction normal to the X-ray beam, as sketched in Figure 2 (a). When the 2-D WAXS pattern is integrated along the radial direction with a narrow q-range (2θ-angle) around the Bragg ring, one can obtain a 1-D azimuthal plot, as presented in Figure 2(c). This can be fitted to a parametric function (such as Maier-Saupe, see [7, 8]) in order to calculate the nematic order parameter (S_2), which is a qualitative measure of the clay particles' orientation distribution. In this case, the S_2 was found to be -0.34 ± 0.02 (remark: $S_2 = 0$ and $S_2 = -0.5$ indicate no preferential orientation and perfect alignment, respectively).

EXPERIMENTAL SET-UP AND ANALYSIS

The experimental set-up is sketched in Figure 3. Castor oil was used as a hosting liquid to fill the cell. The castor oil has a high viscosity (~ 1000 cSt), ensuring that the particles rotate slowly enough to obtain accurate data. The particle is placed in the centre of the cell such that it is completely surrounded by the castor oil. Initially the particle (prepared as described in the sample preparation section) is aligned with the major axis normal to the electric field, and the narrowest side aligned parallel to the electric field. When the field is then applied the particle starts to rotate such that the major axis is eventually aligned parallel to the field. Each measurement is filmed at 30 fps and then the recording is processed using MATLAB by tracking the particle from frame to frame (using the regionprops function). Its angle is calculated by fitting an ellipse to the particle and measuring the angle of the major axis. For each of the measured field strengths the same particle was used, ensuring that the experiments were as similar as possible.

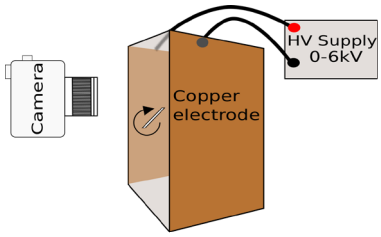

Figure 3: Experimental setup: A video camera is used to film the rotating particle in a glass cell. The two copper electrodes are connected to a high voltage supply capable of supplying up to 5 kV DC. Resulting in an electric field of up to 500 V/mm.

RESULTS AND DISCUSSION

The results for tracking the same particle at different field strengths can be seen in Figure 4. In this plot we see the angle of the particle plotted against the time. It can be clearly seen that the rotation time for the lowest fields (100 V/mm) are considerably longer than for the highest fields (500 V/mm).

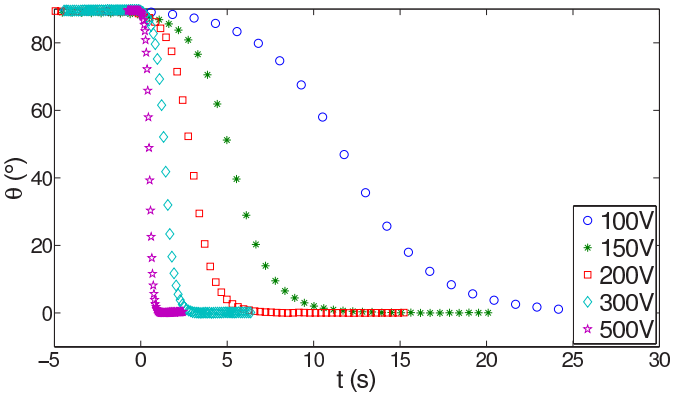

Figure 4: Angle of rotation for a single particle at different electric field strengths. Particle size: $0.85 \times 0.15 \times 0.055$ mm

This is expected as there is an equilibrium between the torque (T) applied from the electric field and the drag of the oil. The torque due to drag in the rotational plane can be written as[9]:

$$T_d = -\zeta_{rot}\dot{\theta}, \tag{1}$$

where ζ_{rot} is the specific rotational drag coefficient in the plane the particle rotates.

The torque due to the electric field is [10,11]

$$\vec{T}_E = (\bar{\chi}\vec{E})\times\vec{E}, \tag{2}$$

which can then be written as

$$T_E = \chi_0 E^2 \sin(\theta)\cos(\theta), \tag{3}$$

where χ_0 is the effective polarizability involving geometric factors. As the data is for the same particle, i.e. the shape and structure are the same, χ_0 is considered a constant.

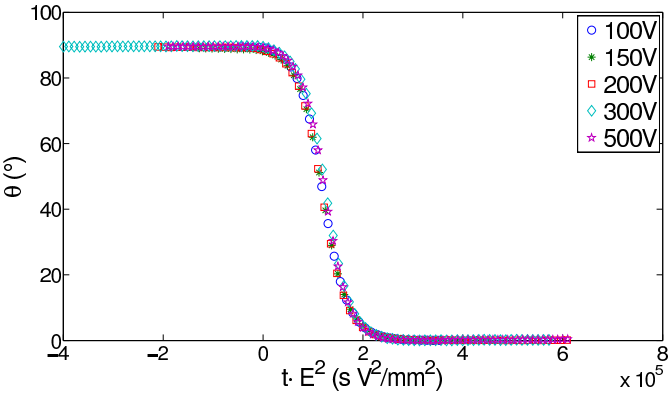

Figure 5: Data collapse of Figure 4, θ plotted against time multiplied by E^2 for different field strengths. Particle size: $0.85 \times 0.15 \times 0.055$ *mm*

We are operating in the low Reynolds number regime ($Re <$ 0.01), and can ignore any inertial effects, hence the electric torque balances the hydrodynamic torque giving

$$\dot{\theta} = -\frac{\chi_0 E^2}{2\zeta_{rot}}\sin(2\theta) = -\frac{1}{2\tau}\sin(2\theta) \tag{4}$$

and thus we obtain

$$\tau \propto \frac{1}{E^2} \tag{5}$$

This is confirmed by way of a data collapse by plotting θ against $t \cdot E^2$, where t is the time and E is the field strength. This can be seen in Figure 5. We should note that we have not treated the anisotropic effects of the dipole that would be encountered as the cylinder rotates. For a more detailed study the reader is referred to Doi and Edwards [9] Solving equation Eq. (4) results in

$$\ln\left(\frac{\tan(\theta)}{\tan(\theta_0)}\right) = -\frac{t-t_0}{\tau}, \tag{6}$$

where t_0 is the time the field is applied, and the corresponding angle $\theta_0 = \theta(t_0)$. We can observe this in Figure 6 where we plot $\ln(\tan(\theta))$ against $t \cdot E^2$ and can see an exponential cut-off, with a slope of -3.4×10^{-5}.

CONCLUSION

From the data we can clearly see that θ scales with time as E^2 as the electric field strength is changed. In future work we wish to determine the effect of the particle geometry, and how multiple water layers affect the rotation time, as in these experiments we only had 1 water layer, and whether the intercalated cations contribute to the dipole moment.

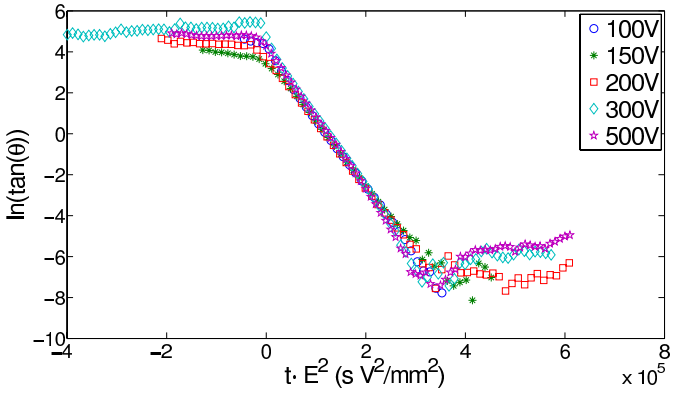

Figure 6: Data collapse of Figure 4, ln (tan (θ)) plotted against time multiplied by E^2 for different field strengths. Particle size: $0.85 \times 0.15 \times 0.055$ *mm*

ACKNOWLEDGEMENTS

This work was supported by the Research Council of Norway through the Nanomat program, project number 182075 and the FRINAT program, project number: 171300.

[1] J. O. Fossum, Y. Méheust, K. P. S. Parmar, K. D. Knudsen, K. J. Måløy and D. M. Fonseca, Europhys. Lett. **74**, 438 (2006).
[2] B. Wang, M. Zhou, Z. Rozynek and J. O. Fossum, J. Mater. Chem. **19**, 1816 (2009).
[3] Z. Rozynek, K. D. Knudsen, J. O. Fossum, Y. Méheust, B. Wang and M. Zhou, J. Phys: Condens. Mat. **22**, 324104 (2008).
[4] Z. Rozynek, H. Mauroy, R. C. Castberg, K. D. Knudsen and J. O. Fossum, Rev. Cub. Fis. **29**, 1E37 (2012).
[5] H. Hemmen, L. R. Alme, J. O. Fossum and Y. Méheust, Phys. Rev. E **82**, 036315 (2010).
[6] P. D. Kaviratna, T. J. Pinnavaia and P. A. Schroeder, J. Phys. Chem. Solids **57**, 1897 (1996).
[7] Y. Méheust, K. D. Knudsen and J. O. Fossum, J. Appl. Cryst. **39**, 661 (2006).
[8] Z. Rozynek, B. Wang, J. O. Fossum and K. D. Knudsen, Eur. Phys. J. E. **35**, 9 (2012).
[9] M. Doi and S. Edwards, *The Theory of Polymer Dynamics*, (Oxford University Press, USA, 1986).
[10] P. Zijlstra, M. van Stee, N. Verhart, Z. Gu and M. Orrit, Phys. Chem. **14**, 4584 (2012).
[11] H-Y Hsu, N. Sharma, R. S. Ruoff and N. A. Patankar, Nanotechnology **16**, 312 (2005).